Potential of Mean Force Computations of Ions Approaching a Surface

ARTICLE *in* LANGMUIR · DECEMBER 2001

Impact Factor: 4.46 · DOI: 10.1021/la015526r · Source: OAI

2 AUTHORS:

Siewert J Marrink
University of Groningen
206 PUBLICATIONS **13,919** CITATIONS
SEE PROFILE

Stjepan Marčelja
Australian National University
60 PUBLICATIONS **4,341** CITATIONS
SEE PROFILE

Potential of Mean Force Computations of Ions Approaching a Surface

Siewert-Jan Marrink* and Stjepan Marčelja

Department of Applied Mathematics, Research School of Physical Science and Engineering, The Australian National University, Canberra, Australia

Received August 8, 2001. In Final Form: October 10, 2001

We present potentials of mean force (PMF) for sodium and chloride ions approaching inert, hydrophobic, and free surfaces under different pressure conditions. The PMFs were obtained from long (10 ns) molecular dynamics simulations in which special care was taken to include all the relevant long-range electrostatic interactions. We find that chloride ions are slightly more repelled close to the surfaces. The range of the ion repulsion is determined mainly by the width of the water/surface interface, a feature which is not captured by electrostatic images.

Introduction

Understanding the interaction between ions in aqueous solutions and interfaces is of fundamental importance to physical chemistry, colloid science, or biology. Because of the complexity of the structure of the aqueous solvent, almost all calculations are presently still performed within the primitive model of electrolytes. An approach promising much improved accuracy is the use of potentials of mean force. Such potentials are now available from simulations for several ion−ion pairs in bulk water (e.g., see refs 1−4). In simple double-layer problems, the use of the potentials of mean force resulted in significant improvements in the computed interaction between two surfaces.[5] However, only a single study[6] addressed the problem of an approach of an ion to the water liquid/vapor interface.

In this paper we present potentials of mean force (PMF) calculations for monovalent ions (sodium and chloride) approaching three different types of surfaces: an inert surface with only a short-range repulsion, a hydrophobic surface with an additional short-range attraction, and a free surface, i.e., the water liquid/vapor interface. The inert wall has no direct physical counterpart and is included here for comparison with theory. The hydrophobic surface mimics a dewetting surface. Note that although the hydrophobic surface is dewetting, it is modeled with a short-range attraction representing dispersive interactions. In comparison to the inert surface therefore, the hydrophobic surface appears slightly hydrophilic. In addition to the data on ion-surface potential of mean force, we also show the data on water depletion layer near a surface. This later topic, first studied by Stillinger[7] using the exact argument based on the contact theorem, is now generating renewed interest because the width and the profile of the surface depletion zone are not well-known.[8]

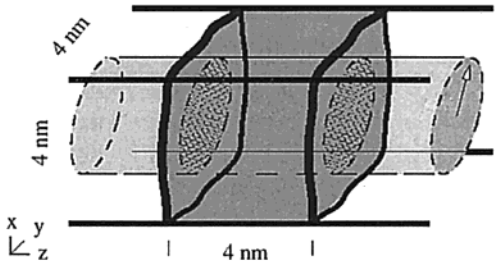

Figure 1. Schematic picture of the system. The water slab is roughly cubic with dimensions of ∼4.0 nm (depending on type of pressure scaling). A cylindrical cutoff scheme was employed using a radius of 1.5 nm. An ion anywhere on the *z* axis at the center of the water slab would interact directly with the water molecules inside the drawn cylinder.

The technique we used to compute the PMFs is molecular dynamics (MD). As we are dealing with charged systems, special care was taken with the treatment of long-range electrostatic interactions. We explicitly analyzed the long-range effect of the ion-induced polarization as well as of the dipolar potential due to orientational ordering of water molecules near the surface. Although some effects proved to be negligible in our system, the approach we took in order to solve this problem could serve as a general model for studying the behavior of charged molecules near interfaces.

The outline of the rest of the paper is as follows. The next section describes the methods used to simulate a slab of water, providing details about the system, the treatment of long-range electrostatic interactions, and the computation of the PMFs. Subsequently, results are presented and discussed. We show the convergence of the long-range dipolar surface correction potential, and for pure water slabs we show the effect of the type of surface on the depletion profiles. Then we turn toward systems containing either a sodium or chloride ion and compare the PMFs for different surfaces. Finally, the main conclusions are summarized.

Methods

2.1. System Details. The geometry of the system is pictured in Figure 1. It consists of a slab of 1728 water molecules and one single ion confined between either two surfaces or two water/vapor interfaces. The two surfaces were modeled by the following potentials (felt by oxygens,

* To whom correspondence should be addressed. Present address: University of Groningen, Department of Biophysical Chemistry, Nijenborgh 4, 9747 AG Groningen, The Netherlands. E-mail: marrink@chem.rug.nl. Fax: 31503634800.

(1) Smith, D.; Dang, L. *J. Chem. Phys.* **1994**, *100*, 3757.
(2) Friedman, R.; Mezei, M. *J. Chem. Phys.* **1994**, *102*, 419.
(3) Guàrdia, E.; Padró, J. *J. Chem. Phys.* **1996**, *104*, 7219.
(4) Lyubartsev, A. P.; Laaksonen, A. *Phys. Rev.* **1997**, *E55*, 5689.
(5) Kjellander, R.; Lyubartsev, A.; Marčelja, S. *J. Chem. Phys.* **2001**, *114*, 9565.
(6) Wilson, M.; Pohorille, A. *J. Chem. Phys.* **1991**, *95*, 6005.
(7) Stillinger, F. H.; Pohorille, A. *J. Solution Chem.* **1973**, *2*, 141.
(8) Lum, K.; Chandler, A.; Weeks, J. D. *J. Phys. Chem.* **1999**, *103*, 4570.

10.1021/la015526r CCC: $20.00
Published on Web 11/09/2001

hydrogens, and the ion)

$$V_1(z) = \epsilon\left[C_r\left(\frac{\sigma}{z}\right)^9 - C_a\left(\frac{\sigma}{z}\right)^3\right] \quad (1)$$

and

$$V_2(z) = \epsilon\left[C_r\left(\frac{\sigma}{d_{surf} - z}\right)^9 - C_a\left(\frac{\sigma}{d_{surf} - z}\right)^3\right]$$

with $\epsilon = 0.5$ kJ/mol and $\sigma = 0.2$ nm. The constant for the repulsive interaction is $C_r = 2/15$, and for the attractive part, $C_a = 1$ modeling a hydrophobic surface or $C_a = 0$ modeling an inert one. These parameters are similar to the ones used in earlier studies of water confinement between walls.[9,10] The surfaces were kept at a fixed distance $d_{surf} = 4.0$ nm. We also performed simulations without a surface, generating two water/vacuum interfaces. In the following "vacuum" is interpreted as the water vapor phase—the density in the vapor phase is so low compared to the bulk phase that it can be neglected.

In the lateral dimensions the system is subject to periodic boundary conditions. To allow the system to relax to bulk densities in the middle of the water slab, lateral pressure coupling was applied in the simulations that included the surfaces. Two types of pressure coupling were compared. In one setup the lateral pressures were coupled to a pressure bath of 1 bar. Due to the surface tension between the water slab and the surface, this results in a large positive pressure (of the order of 150 bar) in the perpendicular direction, i.e., between the slab and the surface. In the other setup we coupled the lateral direction to a pressure with a negative value such that the resulting average perpendicular pressure equaled around 1 bar. In the results section we refer to these cases as the "high pressure" and "low pressure" systems. The pressure coupling in all cases was performed using a weak coupling scheme.[11] In the simulations without a surface, constant area conditions were applied since the water slab has freedom to expand or contract its volume against the vapor. The lateral dimensions in this case were fixed at 4.0 nm. The temperature in all simulations was kept constant using coupling to an external bath of 300 K.[11]

We chose the SPC/E model[12] as our water model. The geometry of the SPC/E molecules was kept rigid using the SETTLE algorithm,[13] allowing a time step of 6 fs.[14] The simulations were performed with the GROMACS simulation software v2.0.[15] An overview of the simulated systems is presented in Table 1.

A Lennard-Jones (LJ) potential models the dispersive and short-range repulsive interactions between the ion and water. The LJ parameters between ion and water (sodium, $\sigma = 0.29$ nm and $\epsilon = 0.20$ kJ/mol; chloride, $\sigma = 0.38$ nm and $\epsilon = 0.54$ kJ/mol) were taken from the standard GROMACS force field.[15]

Both Lennard-Jones and electrostatic interactions were cut off spherically at 1.0 nm, using a group-based scheme.

Table 1. Overview of Simulated Systems[a]

label	surface	P_{lat}	P_z	L
INERT	inert	1	155	3.6
PHOBIC	hydrophobic	1	160	3.5
INERT-low*P*	inert	−130	2	3.8
PHOBIC-low*P*	hydrophobic	−135	5	3.7
VAPOR	none	−200	−12	4.0

[a] Pressures (in bar) and lateral sizes *L* (in nm) are values averaged over 10 ns simulations of pure water systems.

Electrostatic interactions (both water−water and water−ion) with molecules outside of this spherical cutoff were included in two stages: Electrostatic interactions arising from within a larger cylindrical region were updated every 10 time steps and included into the force field. The radius of the cylinder was 1.5 nm, the length of the cylinder equal to the system length (see Figure 1). Interactions from even larger distances were included as external fields, as described in the next two sections.

2.2. Surface Dipolar Layers. With the cylindrical cutoff scheme as outlined above, every atom interacts electrostatically with every other atom in the slab only when the lateral distance between the nearest images is smaller than 1.5 nm. Direct interactions beyond this distance are thus neglected. In bulk water systems, inclusion of electrostatic interactions beyond 1.5 nm does not have any noticeable effect on the system properties. The current system, however, has two surfaces or interfaces, which both create a dipolar potential due to slight preferential ordering of the water molecules. The use of cutoffs neglects the long-range contribution of this dipolar potential. One way of solving the long-range contribution of the surface dipoles would be the use of Ewald summation techniques. Although perfectly suitable for a bulk water slab, the Ewald method is not suitable if an ion is included, as it assumes infinite periodicity of the ionic lattice system. Instead of the approach of a single ion to a surface, the simultaneous approach of many ions would be simulated. Therefore we decided to include the long-range electrostatic contribution of the surface dipoles outside the cylinder as a mean field term in the simulation. The strength of the field can be determined in an iterative way from the simulation of a system without ions, as follows. The electrostatic potential $\Psi(x)$ due to a charge density $\rho(x')$ outside a cylinder of radius R is given by

$$\Psi(x) = 1/(4\pi\epsilon_0)\int\int\int_{V_{cyl}} \frac{\rho(x')}{|x - x'|}\,dx' \quad (2)$$

where ϵ_0 is the dielectric permittivity of vacuum. For a system that is homogeneous in the lateral directions, the above equation can be simplified to[16]

$$\Psi(z) = \frac{1}{2\epsilon_0}\int_{-\infty}^{\infty}\int_{R}^{\infty} \frac{\rho(z')r}{\{(z - z')^2 + r^2\}^{1/2}}\,dr\,dz' + C \quad (3)$$

For a system without net charge

$$\int_{-\infty}^{\infty}\rho(z')\,dz' = 0 \quad (4)$$

and eq 3 reduces to

$$\Psi(z) = -\frac{1}{2\epsilon_0}\int_{-\infty}^{\infty}\rho(z')\{(z - z')^2 + R^2\}^{1/2}\,dz' + C \quad (5)$$

(9) Booth, M.; Du, D.; Haymet, A. *J. Chem. Phys.* **1994**, *101*, 7925.
(10) Spohr, E. *J. Chem. Phys.* **1997**, *106*, 388.
(11) Berendsen, H. J. C.; Postma, J. P. M.; Dinola, A.; Haak, J. R. *J. Chem. Phys.* **1984**, *81*, 3684.
(12) Berendsen, H. J. C.; Grigera, J. R.; Straatsma, T. P. *J. Phys. Chem.* **1987**, *91*, 6269.
(13) Miyamoto, S.; Kollman, P. A. *J. Comput. Chem.* **1992**, *13*, 952.
(14) Feenstra, K. A.; Hess, B.; Berendsen, H. J. C. *J. Comput. Chem.* **1999**, *20*, 786.
(15) Van Der Spoel, D.; Van Buuren, A. R.; Apol, E.; Meulenhoff, P. J.; Tieleman, D. P.; Sijbers, A. L. T. M.; Van Drunen, R.; Berendsen, H. J. C. *Gromacs User Manual Version 1.3*, Nijenborgh 4, 9747 Ag Groningen, The Netherlands. Internet: Http://rugmd0.chem.rug.nl/~gmx, 1996.
(16) Ahlström, P.; Berendsen, H. *J. Phys. Chem.* **1993**, *97*, 13691.

The correction field is obtained through $E(z) = -d\Psi(z)/dz$. The required charge density can be obtained from the simulation

$$\rho(z') = \frac{1}{A}\sum_i q_i \delta(z' - z_i) \tag{6}$$

where A is the lateral system area and the sum runs over all atomic charges q_i. However, the charge density should be obtained from a simulation in which the long-range correction term is already applied. Therefore one needs an iterative procedure to obtain the correct mean field term. The initial charge distribution is computed from a simulation without the additional mean field term. Subsequently, the mean field correction term is computed from the sum over all charges according to eq 5. The simulations are then continued, now including the mean field correction term. A new charge distribution is obtained, from which the procedure can be repeated until the input and output mean field terms have converged. In practice this occurred very rapidly. After one iteration step the input and output charge distributions were already identical within the limits of accuracy.

2.3. Polarization Induced by the Ion. As discussed in the previous section, a cylindrical cutoff scheme was used to incorporate all short- to medium-ranged interactions. The electrostatic interactions between the distant polarization field and water molecules and the ion inside the cylinder were evaluated using classical theory of dielectrics. The electrostatic field is induced by the point charge ion in the slab and an infinite series of its electrostatic images. In calculation of the distant field, water can be treated as a conventional polarizable continuous dielectric rather than the molecular fluid.

The calculation is complicated by the fact that the distant field acts on water molecules anywhere within the cylinder, not just the symmetry axis. Nevertheless, it is quite straightforward. We start by evaluating the polarization field inside the intact slab. In this work we were principally interested in an ion approaching an interface from the inside of bulk water. We therefore considered the long-range field correction due to the polarization by the ion itself and by its nearest image.

Next, we need to evaluate the classical charge density at the surface of the cylinder. The bound surface charge density on the sides, top and bottom of the cylinder is given as $-(\mathbf{P}_2 - \mathbf{P}_1)\cdot\mathbf{n}$, where $\mathbf{P}$ denotes polarization at two sides of the boundary and $\mathbf{n}$ is the normal vector.

In the next stage, we need to calculate the field in the cylinder due to the induced surface charge. It is convenient to use the expression for the electrostatic potential at the position (r,z) due to a charge Q uniformly spread over a ring of the radius R at the position z'

$$V_{\text{ring}}(r,z,R,z') = \frac{1}{4\pi\epsilon_0}\int_0^{\pi} \frac{Q\, d\Theta}{\pi[(z - z')^2 + R^2 + r^2 - 2rR\cos(\Theta)]^{1/2}} \tag{7}$$

This integral can be expressed either in terms of Bessel functions or the elliptic K integral. For the subsequent numerical integration the elliptic integral representation is more convenient because of fast convergence.

Having integrated potential contributions from each ring on the sides, the top, and the bottom of the cylinder, we obtain the electrostatic potential due to the classical polarization field outside of the cylinder. It is now best to differentiate the still analytical integral expression for the potential to obtain the electric field acting on water molecules inside the cylinder. These operations on very long expressions were carried out in Mathematica[17] to save work and avoid errors. Finally tables of the components of electrical fields inside the cylinder were constructed for use in the simulation. A Mathematica notebook using the Macintosh front end containing the details of the calculation is available separately.[18] At this site we also posted images of the correction field for some typical positions of the ion.

The long-range correction field was added to the other force field interactions during the computations of the PMFs. Additional noise introduced at the boundaries of the cylindrical cutoff due to the mean field correction will be taken care off by the heat bath.

2.4. Potential of Mean Force. The PMFs were calculated using the umbrella sampling method.[19] This method adds a biasing potential $U(R)$ to the force field in order to restrict the sampling of the conformational space to a small region around the reaction coordinate R. The reaction coordinate is normally subdivided into a number of overlapping windows, each with its own biasing potential. In our problem, the reaction coordinate forms the position of the ion z_{ion} with respect to the interface. As a biasing potential for the window centered at z_{win}, we choose

$$U(z_{\text{ion}}) = K_1 z_{\text{ion}} + K_2(z_{\text{ion}} - z_{\text{win}})^2 \tag{8}$$

with force constant K_1 set to a window-dependent value and $K_2 = 3000$ kJ mol^{-1} nm^{-2} for $|z_{\text{ion}} - z_{\text{win}}| > 0.3$ nm and $K_2 = 0$ otherwise. The value of K_1 equaled the local slope of the PMF (at z_{win}), estimated from test runs of smaller systems. This choice ensures a more or less even distribution of the ion density across the window. The second term in eq 8 restricts the sampling width for each window to approximately 0.6 nm.

Simulations with the biasing potential added to the ion force field provides the probability density $P(z_{\text{ion}})$ of the ion within the sampled window. From this, the free energy change $A(z_{\text{ion}})$ in each window can be obtained, using

$$A(z_{\text{ion}}) = -kT \ln P(z_{\text{ion}}) - U(z_{\text{ion}}) + C \tag{9}$$

With computation of the statistics in five consecutive windows, each 0.3 nm apart, the PMF for an ion approaching the interface over a distance of 1.5 nm was obtained. The density functions in the 0.3 nm overlap region between two consecutive windows were used to eleminate the unknown constant in eq 9.

The remaining constant has the physical meaning of the free energy of an ion in the center of the slab. In the figures, this was chosen as the zero of the energy scale. Figure 5 also shows the free energy of a point charge in a slab with two classical dielectric boundaries. Such electrostatic image models are traditionally used to calculate the potential of mean force for an ion approaching a surface. We use the classical formula[20] for a point charge in a slab of water surrounded by vacuum.

Results

Before turning to the ion-wall potentials of mean force, we will first show some quantitative details about the

(17) *Mathematica*; W. Research, Inc., 100 Trade Center Drive, Champaign, Il 61820−7237.

(18) Internet: Http://www.rsphysse.anu.edu.au/~stm110/es_corrections.html.

(19) Valleau, J.; Torrie, G. *Statistical Mechanics, Part A: Equilibrium Techniques*; Plenum: New York, 1977.

(20) Barrera, J. G.; Guzmán, O.; Balaguer, B. *Am. J. Phys.* **1978**, *46*, 1172.

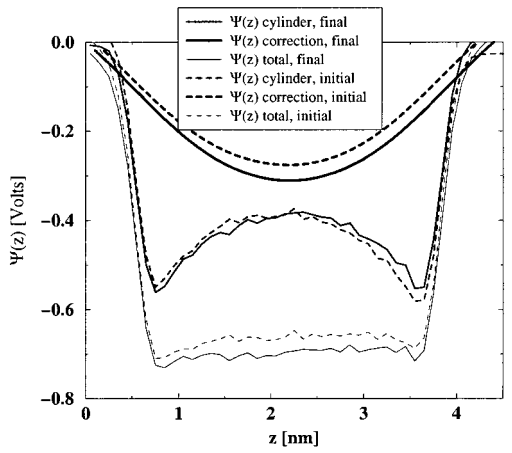

Figure 2. Convergence of the dipolar correction potential. The dipolar correction potential $\Psi^{correction}$, the total dipolar potential Ψ^{total}, and the difference between these two potentials $\Psi^{cylinder}$- are shown before ("initial") and after ("final") one iteration of inclusion of the correction term in the simulation.

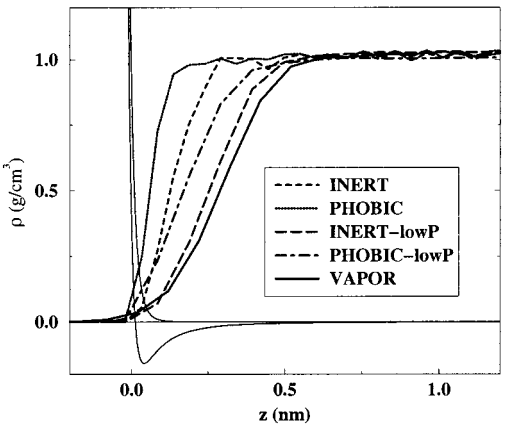

Figure 3. Comparison of interfaces between water and different types of surface: inert, hydrophobic, and vapor. The first two were simulated with negative lateral pressures as well. The potentials modeling the inert and hydrophobic surfaces (eq 1) are also shown.

long-range surface dipolar correction term that we included in our simulations and, subsequently, how the shape of the water/wall interface depends on the type of wall and type of pressure scaling employed.

3.1. Convergence of Long-Range Dipolar Potential. To optimize their hydrogen bonding, water molecules that are confined near an interface tend to order themselves. In simulation studies it is generally found that the ordering is asymmetric—configurations with hydrogens pointing outward the liquid and oxygens inward are slightly more favorable than the other way around. This is observed for water/vapor interfaces[21] as well as for water/hydrophobic type interfaces.[22] Due to this prefential ordering of water molecules near an interface, a dipolar potential will be present in all of our simulations. Using a cutoff scheme for electrostatic interactions during the simulations, the long-range effect of this potential will be lost. To quantify this effect, we have computed the magnitude of the potential contribution from the outside of the cylindrical cutoff according to eq 5. This potential, which is labeled $\Psi^{correction}$ for it is used as a correction term, is shown in Figure 2. We also included the total dipolar potential Ψ^{total}, which one would obtain assuming the simulated charge distribution is representative of an infinite slab of water (i.e., setting $R = 0$ in eq 5), and the difference between these two potentials $\Psi^{cylinder}$, which corresponds to the potential that is actually contributed by the water molecules within the cylindrical cutoff. These three potentials are shown before and after one iteration with the inclusion of the correction term in the actual simulation. The two sets were obtained from 10 ns simulations of a pure water/vapor slab. Similar results were obtained for other systems. As is evident from Figure 2, the contribution of the correction term due to dipolar charges outside the cylinder is of similar magnitude as the contribution from the inside of the cylinder. Nevertheless, the effect of the long-range potential is only small, as the water molecules are able to very effectively screen this potential. One iteration already suffices for convergence of the dipolar correction potential, and it is therefore labeled "final". Subsequent iterations did not improve the convergence any further.

3.2. Shape of Interface. In Figure 3 we compare the profiles of the water/wall interfaces for the five different systems (see Table 1). The results were obtained from 10 ns long simulations of pure water systems. It is clear that the type of interaction between the wall and water as well as the pressure have a large effect on the shape of the interface. Sharpest interfaces are obtained with the hydrophobic wall, which is weakly attractive, unlike the inert or vapor interfaces. At a low lateral pressure a clear dewetting of the surface takes place, and the width of the interface approaches that of the vapor interface. In all cases the profiles are smooth without any clear density oscillations. Explicit trial simulations using other slab geometries for the VAPOR system showed a sharpening of the interface when the lateral system size was reduced. This is caused by the suppression of capillary surfaces waves. Similarly, enlarging the system further broadened the interface. No clear size effects were found for the PHOBIC and INERT systems.

The profile of air/water and surface/water interface has been often calculated in the past. Our result for the free surface is in perfect agreement with ref 23 and slightly broader than the more recent calculation using the same water model with the simulation system sizes of 500 or 1000 molecules.[24]

The profiles of the water/hydrophobic wall interface depend very much on the assumed level of attraction between water and the wall. For a similar wall potential, Spohr[25] found a sharper interface with some oscillatory structure. He used a central force water model, on a much smaller simulation system and over shorter simulation times. We also found oscillatory profiles appearing after short simulation times. However, the profiles are later averaged out over a longer simulation period. The theoretical water/wall profiles of ref 8 are much broader than those found here.

3.3. Potentials of Mean Force. To compute the potentials of mean force for sodium and chloride ions approaching a wall, we applied the following procedure. Initially an ion was inserted into the system by way of replacing one water molecule, near the center of the slab. This was followed by a 100 ps simulation in which the ion was moved toward the interface. Configurations with $z_{ion} = z_{win}$ were selected as the starting configurations of the umbrella sampling runs. For each of the five windows, a 10 ns simulation was performed, enough to obtain precise

(21) Taylor, R.; Dang, L.; Garret, B. *J. Phys. Chem.* **1996**, *100*, 11720.
(22) Van Buuren, A. R.; Marrink, S. J.; Berendsen, H. J. C. *Colloids Surf., A* **1995**, *102*, 143.
(23) Townsend, R. M.; Rice, S. A. *J. Phys. Chem.* **1991**, *94*, 2207.
(24) Sokhan, V. P.; Tildesley, D. J. *Mol. Phys.* **1997**, *92*, 625.
(25) Spohr, E. *J. Phys. Chem.* **1997**, *106*, 3388.

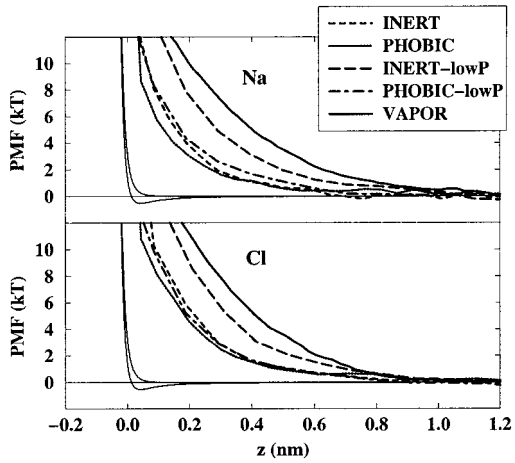

Figure 4. Potentials of mean force for sodium (upper graph) and chloride (lower) for various types of surfaces. The potentials modeling the inert and hydrophobic surfaces (eq 1) are also shown. The zero on the distance scale is chosen as a position where the wall potential is equal to k_BT. In the case of free surface, the zero is selected by matching water density at zero position of the inert surface.

statistics on the probability distributions. The first 200 ps were considered as equilibration in each window and disregarded in the analysis. The inclusion of neither the long-range ion field nor the surface dipolar field appeared to have a significant effect on the probability distributions. Therefore we are confident that the presented results include all the relevant electrostatic interactions. As a further test we sampled two positions of a sodium ion near an INERT surface for a slightly larger system (5 nm in the lateral dimensions) using both a cylindrical cutoff of 1.5 nm and a slightly larger one (1.8 nm). The results appeared independent of system size or cutoff radius. From the simulated probability distributions in the five consecutive windows, the PMF was computed according to eq 9. On the basis of 2 ns subaverages, we estimated a maximum error of 0.4 kT in the resulting PMFs.

It appears that the energy cost for an ion approaching a wall (Figure 4) primarily reflects the decrease in water density. Comparing the results of Figure 4 to the water density profiles in Figure 3 clearly illustrates this similarity. As is the case for the water density profiles, the free energy profiles are also smooth and do not seem to reflect the underlying molecular nature of the solvent. The hydrophobic wall is the least dewetting surface that we have simulated, and the ions can approach closest in the high-pressure simulation. Removing the short range attraction from the hydrophobic wall, i.e., changing to an inert surface, repels the water molecules slightly more and, consequently, the ions as well. In a low-pressure simulation the water/wall surfaces become almost completely dewetting, and the PMFs start to approach the PMF for an interface without a wall, the vapor interface. In this case the interface is very broad with a water density reaching its bulk value over a distance of roughly 0.5 nm. The ions feel the reduced water density and are repelled already at a larger distance.

The reduced density appears to affect the hydration shells of the ion, as seen in a graphical image illustrating the approach of a sodium ion to a surface presented in Figure 5. Similar pictures are obtained for a chloride ion. We show two extreme cases: approach of the least dewetting surface PHOBIC (at high pressure) versus approach of the VAPOR one. The ion is shown at a surface distance corresponding to three different free energy levels,

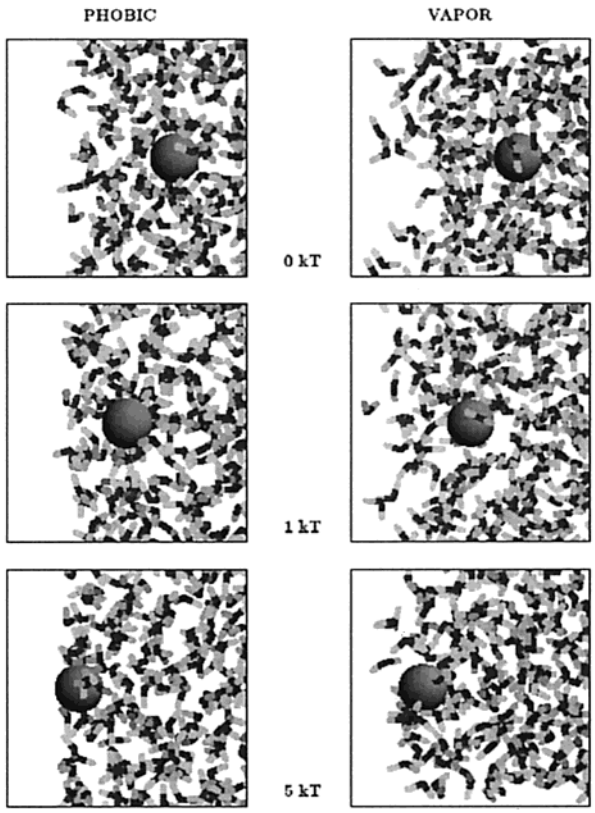

Figure 5. Graphical images of an ion approaching either a high-pressure hydrophobic surface (left) or a vapor interface (right). The free energies of the ions at the chosen positions are 0 kT (upper), 1 kT (middle), and 5 kT (lower).

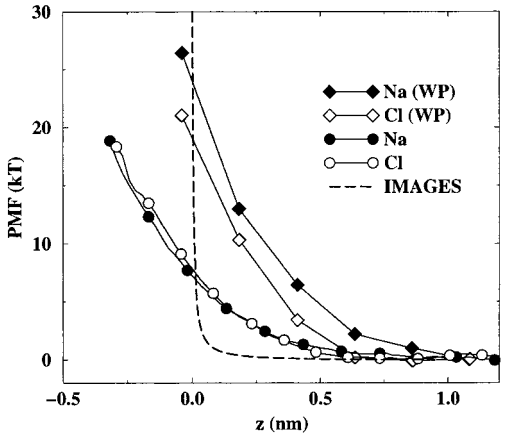

Figure 6. Potentials of mean force for the vapor system calculated in this work, ref 6, and the result for the classical point charge in a dielectric slab.[20] In this figure, zero is defined by the Gibbs dividing surface.

0, 1, and 5 kT. In the images it is apparent that the hydration of the ion is reduced upon approach to the free surface.

In Figure 6 we compare the results just described with the PMF obtained by Wilson and Pohorille[6] and with the classical continuum electrostatics results for a point charge in a dielectric slab. Not surprisingly, the classical result which is based on an infinitely sharp dielectric boundary fails to correctly predict the repulsion felt at shorter distances. Even at distances where the water density has already reached its bulk value, the continuum prediction falls short, pointing to an additional repulsive effect. Two possible explanations are an entropic repulsion due to confinement of intervening water molecules (i.e., a true

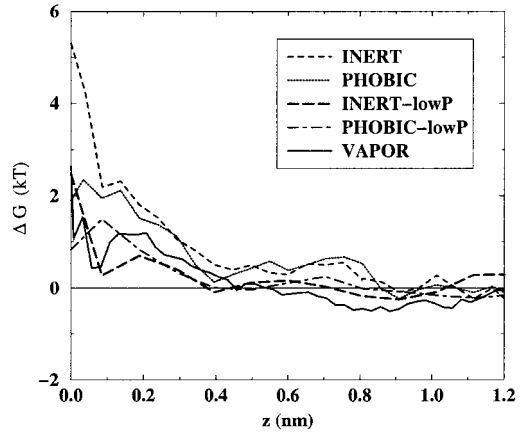

Figure 7. Difference between the potentials of mean force for chloride and sodium, for different surfaces.

hydration force) or an electrostatic repulsion due to the dipolar surface field. Regarding the second mechanism we have already mentioned that the surface dipolar field does not significantly change values of PMF. In addition, any electrostatic field would have an opposite effect on sodium versus chloride ions. One would expect a repulsion for sodium, whereas chloride should be attracted by the dipolar field. In Figure 7, where we plotted the differences between the PMFs of sodium and chloride, we show that this is not the case. On the contrary, close to the surface chloride ions seem to be repelled more than sodium ions for each of the surface types studied. The difference appears to be somewhat larger for the systems which possess the sharpest interfaces (PHOBIC and INERT). Further away (at distances larger than $\approx$0.4 nm) there is no longer a significant difference between the PMF for sodium and chloride. This observation is in contrast to the results of the earlier simulations by Wilson and Pohorille.[6] They observed a stronger repulsion from a water/vapor interface of sodium compared to either chloride or fluoride at distances larger than 0.5 nm.

Although generally similar, the results of ref 6 do not agree well with our findings (Figure 6). Their water model (TIP4P) is different, but more likely the source of discrepancy is their use of a short spherical cutoff for electrostatic interactions between the ion and water (1.0 nm) which might have a large influence.

Conclusion

Detailed molecular dynamics simulations including all the relevant long-range electrostatic interactions have resulted in accurate potentials of mean force for both sodium and chloride ions approaching an inert surface, a hydrophobic surface, and a free surface. We found that the potentials of mean force primarily reflect the density profiles of the water molecules, which are sensitive to the value of pressure in the system. For the surfaces studied, the density profiles are smoothly decaying and we do not find any structuring effects in the PMFs either. Standard mean field predictions based on sharp dielectric boundaries clearly underestimate the ion repulsion. We observed only a minor difference between the surface repulsion of sodium versus chloride. At very close distances chloride is repelled somewhat stronger, irrespective of the type of surface.

Acknowledgment. S.J.M. acknowledges support from The Netherlands Organization for Pure Research, NWO.

LA015526R